All-fiber Yb:fiber frequency comb

Yawei Chang (常亚伟), Tongxiao Jiang (姜通晓), Zhigang Zhang (张志刚), and Aimin Wang (王爱民)*

State Key Laboratory of Advanced Optical Communication System and Networks, School of Electronics, Engineering and Computer Science, Peking University, Beijing 100871, China

**Corresponding author: wangaimin@pku.edu.cn*

Received November 16, 2018; accepted March 1, 2019; posted online May 17, 2019

We demonstrate an all-fiber Yb:fiber frequency comb with a nonlinear-amplifying-loop-mirror-based Yb:fiber laser oscillator. The fiber-spliced hollow-core photonic bandgap fiber was used as dispersion compensator, which was also directly spliced to a piece of tapered photonic crystal fiber for an octave-spanning spectrum. The spectrum of the compressed 107 fs laser pulses was broadened, covering 600 nm to 1300 nm in a high-nonlinearity tapered fiber for f to $2f$ beating. The signal-to-noise ratio of offset frequency was measured to be 22 dB.

OCIS codes: 320.7090, 140.3510.
doi: 10.3788/COL201917.053201.

For building frequency combs, fiber lasers have attracted a lot of attention due to their high efficiency, high power, low cost, and especially high integration with an all-fiber configuration[1,2]. Er:fiber laser frequency combs have demonstrated their advantages with an all-fiber structure[3]. Compared to Er:fiber laser frequency combs, Yb:fiber lasers can supply higher power, and their wavelength is closer to the visible wavelengths, especially required for some applications, such as astronomical spectroscopy, optical clock, and biology imaging[4,5]. The repetition frequency and carrier envelop offset frequency (f_{ceo}) are two important parameters in a comb, and we can get the f_{ceo} by f to $2f$ beating. However, the fully stabilized laser frequency combs with locked f_{ceo} are quite sensitive to the environment. Especially, limited by the dispersion elements, Yb:fiber laser frequency combs still contain many bulk components, such as grating pairs for dispersion compensation and free space coupling of photonic crystal fibers (PCFs). All of these free space components can cause the instability of the comb and limit the comb applications. Although all-fiber Yb:fiber laser combs should be the best solution, so far, not much progress has been reported.

The commonly used mode-locking mechanism in a laser comb includes the nonlinear polarization evolution (NPE), semiconductor saturable absorber mirror (SESAM) and carbon nanotube saturable absorber (CNT SA) based mode locking[6,7]. NPE-based fiber lasers are sensitive to the environment, and SESAM-based ones are easy to break down due to their low damage threshold. Fiber lasers based on a nonlinear amplifying loop mirror (NALM) have received lots of attention in recent years due to their high stability and low self-start threshold[8,9], especially using polarization maintaining (PM) fibers. PCFs with abnormal dispersion have been proved to be one of the best candidates for replacing some free-space optical elements, such as grating and prism pairs, for compensation components[10,11]. In a Yb:fiber laser comb, there are at least two free-space pulse compression components that can be replaced by PCFs: the intracavity and the extracavity pulse compression. Because we need to control the cavity length and cavity dispersion adjustment in a frequency comb, we retain the intracavity space elements as grating pairs and a mirror. For the extracavity pulse compression, the amplified pulse may have a very high peak power, and the hollow-core (HC) photonic bandgap fiber (PBGF) is preferred to replace the grating pairs due to its low high-order dispersion and high-power handling[11].

To obtain the octave-spanning spectrum with low pulse energy, we have already developed and applied the technique of tapered PCFs[12,13]. Since the entrance core diameter is not as small as the tapered part, the mode matching and fiber splicing will be easier.

In this Letter, we demonstrated a stable all-PM-fiber Yb:fiber laser frequency comb, which employed two different kinds of PCFs. By splicing the HC-PBGF and tapered PCF together[14], the compressed pulses were directly launched into the tapered PCFs. The comb can be considered as a performance of the all-fiber Yb frequency comb, showing the potential for extended applications.

The schematic of the all-fiber optical frequency comb is shown in Fig. 1. The oscillator was a PM Yb:fiber cavity running on the NALM structure, which consists of a nonlinear loop and a linear arm. The grating pairs in the linear arm help to optimize the intracavity dispersion that has a great impact on the linewidth of the carrier envelope offset signal (f_{ceo}). Output 1 worked as a seed source for the latter amplification and output 2 as a monitor. Output 3 was shelved due to its undesirable spectrum.

When the pump power was higher than 700 mW, the oscillator can self-start but work at the multiple-pulse regime. We obtained the single-pulse operation when the pump power was slowly decreasing to 240 mW. The Yb:fiber laser worked at the repetition rate of 102 MHz centered at 1037 nm. The cavity dispersion was estimated to be -1100 fs^2.

We used a piezoelectric ceramic transducer (PZT) mounted with a mirror to keep the cavity length stable.

 © 2019 Chinese Optics Letters

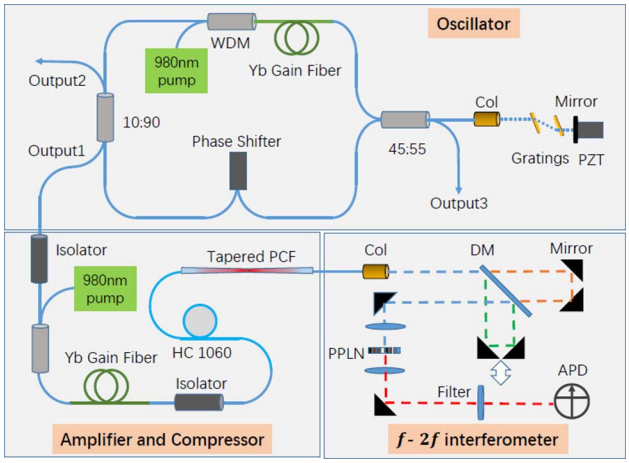

Fig. 1. Schematic of the integrated all-fiber Yb:fiber laser frequency comb system. WDM, wavelength division multiplexer; PZT, piezoelectric ceramic transducer; DM, dichroic mirror; PCF, photonic crystal fiber; PPLN, periodically poled lithium niobate; APD, avalanche photodiode.

We locked the repetition frequency through an electrical control system. The repetition frequency can be locked for more than 10 h with the standard deviation of the repetition frequency of 0.22 mHz and fractional frequency instability of $2.4 \times 10^{-12}\,\mathrm{s}^{-1}$, which are shown in Figs. 2(a) and 2(b).

The average power of output 1 was about 1.5 mW, and it was amplified to about 400 mW by a single-mode PM Yb-doped fiber (PM-YSF-HI) at the pump power of 900 mW. The pulse spectra of output 1 (red) and after the amplifier (black) are given in Fig. 2(c). The wavelength span of the spectrum was broadened from 6 to 27 nm because of the nonlinear effects of the gain fiber and the single-mode PM 980 fiber. It is obviously exhibiting a blue shift during the amplification.

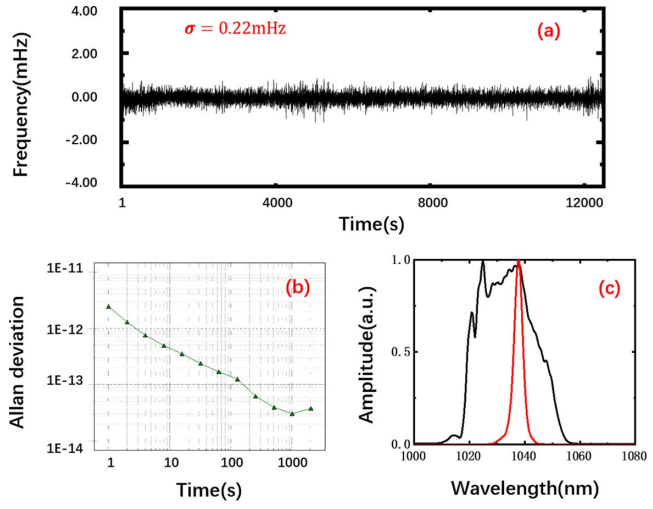

Fig. 2. (a) Residual fluctuations of the repetition frequency; (b) the Allan deviation calculated by data shown in (a); (c) the spectra of the oscillator (red line) and after the amplifier (black line).

An HC-PBGF [HC 1060, from NKT Ltd., with the mode field diameter (MFD) of ~7.5 μm] was used for pulse compression. The splicing loss between amplifier pigtail and HC 1060 can be optimized to lower than 2 dB by adjusting the splicing current and duration time of the splicer (Fujikura FSM-100 P+). Another tapered high-nonlinearity PCF (HN-PCF, with the core size of ~4.6 μm) was spliced to the output end of the HC fiber for supercontinuum generation. The end faces of these two kinds of PCFs from scanning electron microscope (SEM) images are given in Figs. 3(a) and 3(b). Due to the hollow and different fiber structure of the two fibers, both fibers around the splicing point collapse seriously in a direct splicing way, leading to the splicing loss that is always over 4 dB. To reduce the splicing loss, a bridge fiber (Corning HI1060) with an MFD of 6.5 μm was used to connect them together, as shown in Fig. 3(c). The MFD of HI 1060 is close to the MFD of HC 1060, which can maintain less splicing loss. Because the HN-PCF is not as easy to collapse as HC 1060, we can get a very low loss between the HI 1060 and HN-PCF. By finely controlling the discharge current and duration time of the splicer, the splicing loss can be enhanced to below 3 dB, which was close to the efficiency of spatial coupling. The length of HI 1060 was shorter than 10 mm, and we can protect the two splicing points together by one heat shrink tube. Our comb contains no space element from the oscillator to spectrum broadening region, which has the ability to make the system more stable and integrated.

A 107 fs pulse was obtained after a 4.1 m HC-PCF, with the autocorrelation trace shown in Fig. 3(d). The pulse wings are not quite clean due to the adjustment difficulties of the hollow fiber length.

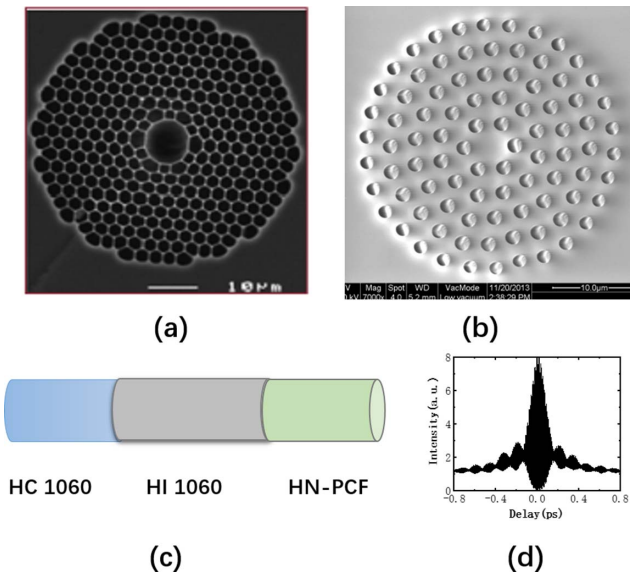

Fig. 3. (a) End face of NKT HC 1060 fiber by SEM from NKT photonics; (b) end face of HN-PCF by SEM; (c) fiber HI 1060 acts as bridge fiber to connect the two PCFs together with loss less than 3 dB; (d) measured autocorrelation trace of the pulses compressed by HC PCF.

A tapered HN-PCF, which has a similar structure with the tapered PCFs in Refs. [11,12], was used for supercontinuum generation. The original core diameter of the HN-PCF is 4.6 μm with the d/Λ ratio of 0.53. The core diameter is tapered to 1.8 μm, resulting in the nonlinearity coefficient increasing from 11 to 74.5 $W^{-1} \cdot km^{-1}$. The original HN-PCF has only one zero dispersion wavelength (ZDW) at 1018 nm, while the tapered HN-PCF has two ZDWs at 794 and 1129 nm, and the pump laser wavelength was in the anomalous dispersion region between the two ZDWs[12]. The tapered length is about 5 cm, and the transition area lengths are 3 cm long, respectively, on both sides of the fiber.

The octave-spanning spectrum generated in the tapered HN-PCF is shown in Fig. 4(a), which covers from 600 to 1300 nm. The generated octave-spanning spectrum is broad enough and has an appropriate frequency pair for f_{ceo} signal detection.

The spectral components at 630 and 1260 nm in the octave-spanning spectrum were used for the f_{ceo} beating. Before the beating, the fundamental wavelength and the frequency-doubled pulses were separated by a dichroic mirror (DM) and recombined after an optical delay line for the delay compensation. A periodically poled lithium niobate (PPLN) crystal was used for frequency doubling of 1260 nm wavelength pulses. The fundamental and the second harmonic pulses were sent through a bandpass filter centered at 630 nm and then onto the silica avalanche photodiode (APD). The intracavity grating pairs' distance and amplification pump power were slightly adjusted for better f_{ceo} signal. The f_{ceo} beat signal-to-noise ratio (SNR) was measured to be 22 dB [with the resolution bandwidth (RBW) = 300 kHz], as shown in Fig. 4(b).

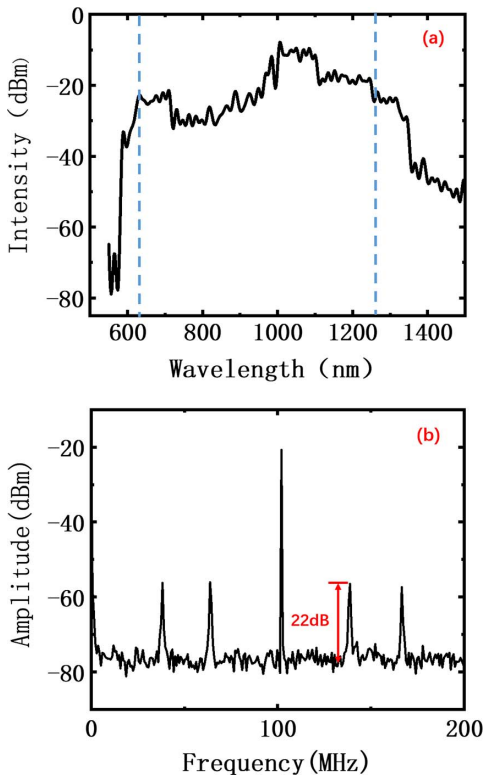

Fig. 4. (a) The experiment (black line) octave-spanning spectrum generated from HN-PCF; (b) the f_{ceo} signal detected from the APD at the resolution bandwidth of 300 kHz.

In conclusion, we demonstrated an integrated 102 MHz Yb:fiber laser frequency comb in an all-fiber structure, using a hollow fiber to replace the free-space dispersion compensation grating pairs. It contained no free-space element from the oscillator output to the spectrum broadening part by splicing PCFs together to make the system more stable and integrated. The offset frequency f_{ceo} signal was detected with 22 dB SNR at 300 kHz RWB. The offset frequency locking will be reported in a future study.

Although the comb has become more compact by employing a near all-fiber NALM structure and splicing two PCFs together, there is still room for improvement. First, the oscillator can be more stable with a compact mechanical design and by adding a temperature control module. Second, we can optimize the pulse width for offset frequency locking in a future study. Furthermore, the Michelson interferometer should be removed by a well-designed tapered PCF that could be able to compensate the delay between the fundamental and the second harmonic wave. This relies on our further design and fabrication of the PCF.

This work was supported by the National Key R&D Program of China (No. 2016YFF0200204) and the National Natural Science Foundation of China (Nos. 31327901 and 61475008).

References

1. M. E. Fermann and I. Hartl, Nat. Photon. **7**, 868 (2013).
2. M. E. Fermann and I. Hartl, IEEE J. Sel. Top. Quant. **15**, 191 (2009).
3. B. R. Washburn, S. A. Diddams, N. R. Newbury, J. W. Nicholson, M. F. Yan, and C. G. Jorgensen, Opt. Lett. **29**, 250 (2004).
4. T. Ideguchi, S. Holzner, B. Bernhardt, G. Guelachvili, N. Picqué, and T. W. Hänsch, Nature, **502**, 355 (2013).
5. T. Wilken, C. Lovis, A. Manescau, T. Steinmetz, L. Pasquini, G. Lo Curto, T. W. Hänsch, R. Holzwarth, and T. Udem, Mon. Not. R. Astron. Soc. **405**, L16 (2010).
6. X. Liu, X. Yao, and Y. Cui, Phys. Rev. Lett. **121**, 023905 (2018).
7. J. Peng and H. Zeng, Laser Photon. Rev. **12**, 1800009 (2018).
8. G. Liu, A. Wang, and Z. Zhang, IEEE Photon. Technol. Lett. **29**, 23 (2017).
9. Y. Li, N. Kuse, A. Rolland, Y. Stepanenko, C. Radzewicz, and M. E. Fermann, Opt. Express **25**, 15 (2017).
10. P. Russell, J. Lightwave Technol. **24**, 4729 (2006).
11. T. Jiang, A. Wang, W. Zhang, F. Niu, G. Wang, C. Li, and Z. Zhang, in *CLEO: QELS_Fundamental Science* (Optical Society of America, 2014), paper JW2A.6.
12. T. Jiang, A. Wang, G. Wang, W. Zhang, F. Niu, C. Li, and Z. Zhang, Opt. Express **22**, 1835 (2014).
13. G. Wang, F. Meng, C. Li, T. Jiang, A. Wang, Z. Fang, and Z. Zhang, Opt. Lett. **39**, 2534 (2014).
14. X. Liu, J. Lægsgaard, U. Moller, H. Tu, S. A. Boppart, and D. Turchinovich, Opt. Lett. **37**, 2769 (2012).